Nonlinear Phenomena in Erbium-Doped Lasers

Andreea Sterian and Valerică Ninulescu

Department of Physics, "Politehnica" University of Bucharest,
Splaiul Independenţei 313, Bucharest, 060042, Romania
vninul@physics.pub.ro

Abstract. The nonlinear dynamics of an erbium-doped fiber laser is explained based on a simple model of the ion pairs present in heavily doped fibers. The single-mode laser dynamics is reductible to four coupled nonlinear differential equations. Depending on the ion-pair concentration, the pumping level and the photon lifetime in the laser cavity, numerical calculations predict cw, self-pulsing and sinusoidal dynamics. The regions of these dynamics in the space of the laser parameters are determined.

1 Introduction

In recent years much attention has been paid to the study of nonlinear effects in optical fibers [1, 2, 3, 4, 5, 6]. Erbium-doped fiber lasers (EDFLs) present numerous applications in telecommunications and laser engineering. In the same time, it is also a promising system for theoretical nonlinear studies [7, 8]. Self-pulsing and chaotic operation of the EDFLs has been reported in various experimental conditions [3, 4], including the case of pumping near the laser threshold. We present a model for the single-mode laser taking into account the presence of the erbium ion pairs that act as a saturable absorber.

2 The Basic Model

The erbium-doped laser emitting around 1.55 μm ($^4I_{13/2} \to {}^4I_{15/2}$ transition) is a three-level system (Fig. 1). Er^{3+}-ions at a concentration N_0 are pumped with the rate Λ from level 1 ($^4I_{15/2}$) to level 3 (for example $^4I_{11/2}$, 980 nm above the ground state). The level 3 is fastly depopulated through a non-radiative transition on the upper laser level 2 ($^4I_{13/2}$) which is metastable with the lifetime $\tau_2 = 1/\gamma_2 = 10\,\mathrm{ms}$. The letter σ in Fig. 1 denotes the absorption cross section in the laser transition. In the rate equation approximation, the laser dynamics is described based on two coupled differential equations, one for the population inversion and the other for the laser intensity:

$$\frac{\mathrm{d}n}{\mathrm{d}t} = 2\Lambda - \gamma_2(1+n) - 2in \ , \tag{1}$$

$$\frac{\mathrm{d}i}{\mathrm{d}t} = -i + Ain \ . \tag{2}$$

O. Gervasi et al. (Eds.): ICCSA 2005, LNCS 3482, pp. 643–650, 2005.

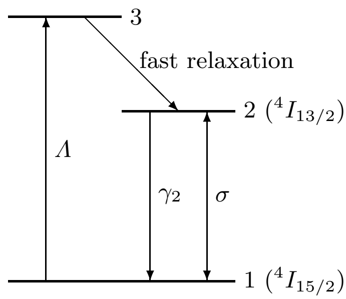

Fig. 1. Erbium-ion energy levels implied in the laser effect

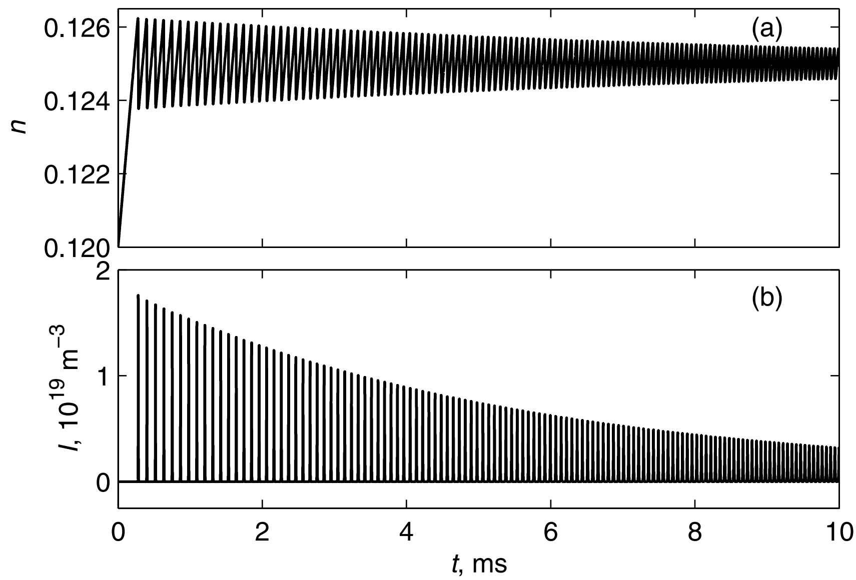

Fig. 2. Transient dynamics of the erbium laser. (a) Population inversion; (b) Laser intensity. Numerical values of the laser are given in text and photon lifetime is $\tau = 10^{-8}$ s. The plot starts at a point where the population inversion reaches a value close to the stationary one

Here, the time is expressed in units of the photon lifetime τ in the laser cavity, $n = n_2 - n_1$ is the difference of the occupation probability of level 1 and 2, respectively, and i stands for the dimensionless laser intensity; $i = \sigma I \tau$, where I denotes the photon density of the laser field. The parameter A in Eq. (2) is $A = \sigma N_0 \tau$; note that parameter γ_2 in Eq. (1) is dimensionless, i.e., the relaxation rate is expressed in $1/\tau$ units.

The determination of the steady-states furnishes the points

$$n = 2\Lambda/\gamma_2 - 1,\ i = 0 \quad \text{and} \quad n = 1/A,\ i = A(\Lambda - \Lambda_{\text{th}})\ , \tag{3}$$

where

$$\Lambda_{\mathrm{th}} = \frac{\gamma_2}{2}\left(1 + \frac{1}{A}\right) . \tag{4}$$

Linear stability investigation gives laser action for $\Lambda > \Lambda_{\mathrm{th}}$ and the laser solution is stable for all pumping levels above threshold. Concerning the type of stability, we notice that the eigenvalues λ of the linearized system around the laser solution,

$$\lambda^2 + 2A\left(\Lambda - \frac{A}{A+1}\Lambda_{\mathrm{th}}\right)\lambda + 2A(\Lambda - \Lambda_{\mathrm{th}}) = 0 \ , \tag{5}$$

can be both negative (node) or complex-conjugate with negative real part (focus). We take $N_0 = 5 \times 10^{24}\,\mathrm{m}^{-3}$, $\sigma = 1.6 \times 10^{-16}\,\mathrm{m}^3\mathrm{s}^{-1}$ and $\tau = (2 \div 200)\,\mathrm{ns}$. In terms of the pumping strength $r = \Lambda/\Lambda_{\mathrm{th}}$, the changes in the stability type occur for $r_- = 1 + A\Lambda_{\mathrm{th}}/2(A+1)^2 \approx 1$ and $r_+ = 1 + 2/A\Lambda_{\mathrm{th}} \gg 1$. Practically, for all accessible pumping levels and all photon lifetimes, the eigenvalues are complex conjugate; consequently, the approaching to the stable laser solution is performed through relaxation oscillations (Fig. 2).

3 Ion-Pair Influence

At sufficiently large ion concentrations, their interaction gives rise to clusters with a distinct contribution to the laser effect. One model considers the amplifying medium as a mixture of isolated erbium ions and erbium ion pairs [3]. The strength of the interaction in an ion-pair is relatively small due to the screening effect of the $4d^{10}$ electrons on the $4f$ electrons. So, the ion energy levels are practically preserved and the energy in an ion-pair is the sum of the two ions energy. The ion-pair importance is related to the quasiresonance of the transition ${}^4I_{9/2} \to {}^4I_{13/2}$ with the laser transition. This makes it probable the up-conversion process in an ion-pair (Fig. 3). For an ion-pair the laser levels are 11 (ground level), 12 (intermediate level) and 22 (uppermost level), separated through the laser transition. Denoting by n_{11}, n_{12} and n_{22} the corresponding populations, these quantities satisfy the normalization condition $n_{11} + n_{12} + n_{22} = 1$.

Based on the above picture of the active medium, two supplementary equations are to be added to Eqs. (1,2). By use of the new variables $n_\pm = n_{22} \pm n_{11}$, the complete set of laser equations is

$$\frac{\mathrm{d}n}{\mathrm{d}t} = 2\Lambda - \gamma_2(1+n) - 2in \ , \tag{6}$$

$$\frac{\mathrm{d}n_+}{\mathrm{d}t} = \gamma_2(1-n_+) - \frac{\gamma_{22}}{2}(n_+ + n_-) + yi(2 - 3n_+) \ , \tag{7}$$

$$\frac{\mathrm{d}n_-}{\mathrm{d}t} = 2\Lambda - \gamma_2(1-n_+) - \frac{\gamma_{22}}{2}(n_+ + n_-) - yin_- \ , \tag{8}$$

$$\frac{\mathrm{d}i}{\mathrm{d}t} = -i + (1-2x)Ain + xAyin_- \ . \tag{9}$$

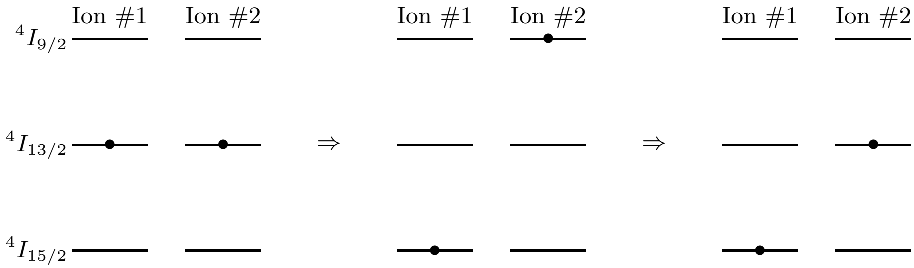

Fig. 3. Up-conversion (*center*) followed by relaxation (*right*) in an ion-pair

The quantity x is the fraction of ion pairs in the active medium, γ_{22} is the (reduced) relaxation rate of levels 22 and 12, and $y\sigma$ $(0 < y < 1)$ is the absorption cross section for the laser transition in an ion-pair.

4 Steady-States

The determination of the steady-states of system (6)–(9) reduces to the solutioning of a third-order polynomial equation for the laser intensity; this is

$$i^3 + c_1 i^2 + c_2 i + c_3 = 0 \ , \tag{10}$$

where

$$c_1 = Ax(\gamma_{22} - 2\gamma_2)/3 + (\gamma_2 + 2\gamma_{22})/3y + \gamma_2/2 - A(2\Lambda - \gamma_2)/2 \ , \tag{11}$$

$$\begin{aligned} c_2 = {} & x[A\gamma_2(\gamma_2/6 + \gamma_{22}/6 - \Lambda) + A\gamma_{22}\Lambda/y - A\gamma_2(\gamma_2 + \gamma_{22})/3y] \\ & + \gamma_2(\gamma_2 + 2\gamma_{22})/6y + \gamma_2\gamma_{22}/3y^2 - A(\gamma_2 + 2\gamma_{22})(2\Lambda - \gamma_2)/6y \ , \end{aligned} \tag{12}$$

$$\begin{aligned} c_3 = {} & Ax\gamma_2(\gamma_2\gamma_{22} - 2\gamma_2\Lambda - \gamma_{22}\Lambda)/6y + \gamma_2^2\gamma_{22}/6y^2 \\ & - A(1 - 2x)\gamma_2\gamma_{22}(2\Lambda - \gamma_2)/6y^2 \ . \end{aligned} \tag{13}$$

The laser threshold is obtained from the condition $c_3 = 0$ that yields

$$\Lambda_{\mathrm{th}} = \frac{1 - Ax(2 - y)/(A + 1)}{1 - (2 - y/2 - y\gamma_2/\gamma_{22})x}\Lambda_{\mathrm{th}}^0 \ , \tag{14}$$

where Λ_{th}^0 is the pump threshold in the absence of the ion pairs and it is given by Eq. (4). Besides previously given laser parameters, we take the lifetime $\tau_{22} = 2\,\mu\mathrm{s}$ of the ion-pair level 22 and $y = 0.2$. The dependence of the threshold pumping level on the concentration of the ion-pair and the photon lifetime is presented in Fig. 4. The increase of the laser threshold due to the presence of the ion pairs is an important drawback of heavily doped fibers.

Above threshold, there exists only one steady-state laser intensity given by Eq. (10), the other two being unphysical (negative). The numerical calculation of the steady-state intensity for a significant range of the pumping parameter gives a laser intensity following a straight line dependency (Fig. 5) as in the absence of the ion pairs [see Eq. (3)].

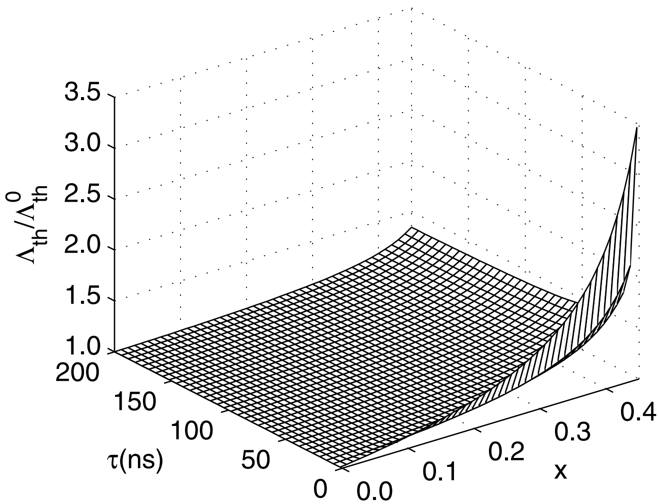

Fig. 4. Threshold pumping parameter vs. ion-pair percentage and photon lifetime. The laser parameters are given in text

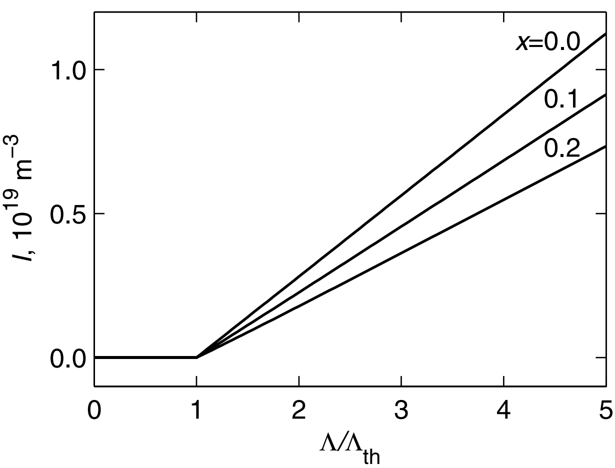

Fig. 5. Steady-state photon density of the laser field vs. the pumping strength $\Lambda/\Lambda_{\mathrm{th}}$. The same parameters as in Fig. 4 and $\tau = 10^{-8}\,\mathrm{s}$

5 Laser Dynamics

Linear stability investigation of the steady-states [7, 8] reveals the existence of a critical value of the ion-pair percentage under which the steady-state (cw) solution is stable whatever the pumping level. At larger concentrations of the ion pairs, the laser is in a steady-state or self-pulsing, depending on the value

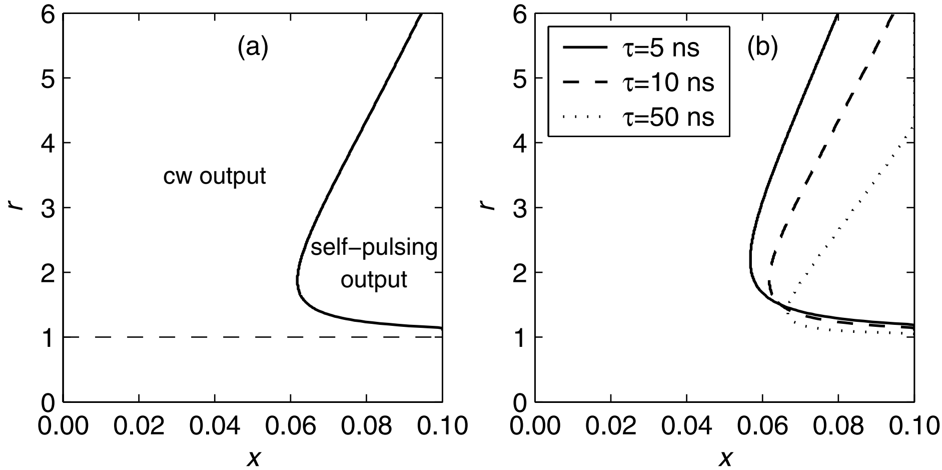

Fig. 6. (a) Calculated stability diagram for the EDFL. $\tau = 10\,\text{ns}$; (b) The influence of the photon lifetime on the margins of the stability domains

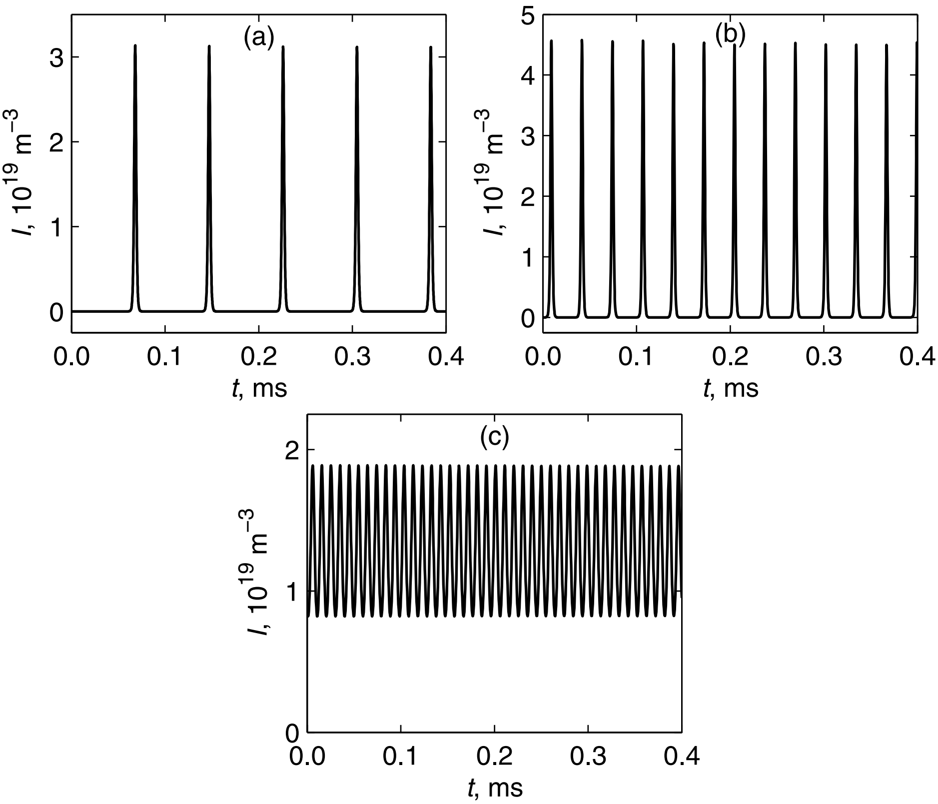

Fig. 7. Asymptotic temporal evolution of the photon density for a fraction $x = 0.1$ of ion pairs and the pumping level (a) $r = 1.5$, (b) $r = 2.5$, and (c) $r = 6.6$. $\tau = 10^{-8}\,\text{s}$

of the pumping parameter $r = \Lambda/\Lambda_{\mathrm{th}}$ [Fig. 6(a)]. The transition from the cw dynamics to a self-pulsing one takes place when two complex conjugate eigenvalues of the linearized system cross the imaginary axis from left to right, i.e., a Hopf bifurcation occurs [7]; in such conditions the steady-state solution becomes unstable and the long term system evolution settles down on a stable limit cycle in the phase space. Figure 6(a) shows that the low branch of the Hopf bifurcation corresponds to pumping strengths close to the threshold value.

The quantitative changes of the laser intensity inside the self-pulsing domain are clarified in Fig. 7. At a fixed value of the ion-pair concentration, the increase in pumping gives rise to pulses of a higher repetition rate and close to the bifurcation point the intensity becomes sinusoidal. Besides, pulse amplitude reaches a maximum approximately in the middle of the self-pulsing domain.

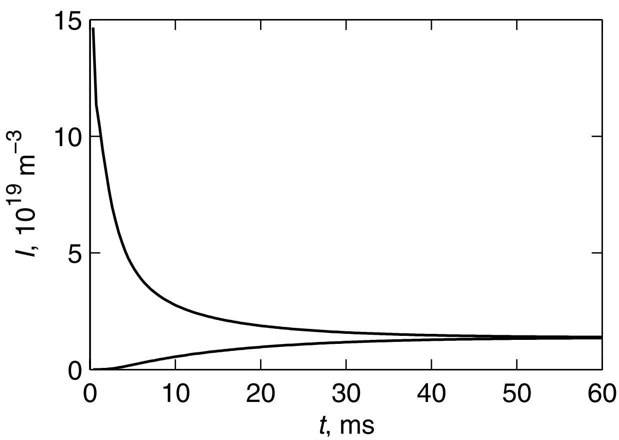

Fig. 8. Envelope of the transient photon density for a pumping parameter $r = 7$. The same laser parameters as in Fig. 7

Further increase of the pumping strength gives again a cw dynamics (Fig. 8).

The photon lifetime contribution to the stability diagram is emphasized in Fig. 6(b). This proves that cavities with low losses makes it possible to preserve the cw dynamics even at larger doping levels.

6 Conclusion

The erbium ion pairs in a fiber laser can explain the experimentally observed nonlinear dynamics of the system [2, 3]. In the single-mode laser description, the ion pairs are responsible for an increase of the laser threshold and a decrease of the laser power, and self-pulsations. Depending on the experimental conditions, the laser self-pulsations range from an oscillatory form to a well defined pulse-shape. The nonlinear dynamics can be limited by a choice of sufficiently low doped fibers at the expense of using longer fibers.

References

1. Agrawal, G. P.: Nonlinear Fiber Optics. 2nd edn. Academic Press, San Diego (1995)
2. LeFlohic, M., François, P.L., Allain, J.Y., Sanchez, F., Stephan, G.: Dynamics of the Transient Buildup of Emission in Nd^{3+} Doped Fiber Lasers. IEEE J. Quantum Electron. **27** (1991) 1910–1921
3. Sanchez, F., LeBoudec, P., François, P.L., Stephan, G.: Effects of Ion Pairs on the Dynamics of Erbium-Doped Fiber Lasers. Phys. Rev. A **48** (1993) 2220–2229
4. Sanchez, F., LeFlohic, M., Stephan, G.M., LeBoudec, P., François, P.L.: Quasi-Periodic Route to Chaos in Erbium-Doped Fiber Laser. IEEE J. Quantum Electron. **31** (1995) 481–488
5. Williams, Q.L., García-Ojalvo, J., Roy, R.: Fast Intracavity Polarization Dynamics of an Erbium-Doped Fiber Ring Laser: Inclusion of Stochastic Effects. Phys. Rev. A **55** (1997) 2376–2386
6. DeShazer, D.J., García-Ojalvo, J., Roy, R.: Bursting Dynamics of a Fiber Laser with an Injected Signal. Phys. Rev. E **67** (2003) 036602
7. Crawford, J.D.: Introduction to Bifurcation Theory. Rev. Mod. Phys. **63** (1991) 991–1037
8. Abarbanel, H.D.I., Brown, R., Sidorowich, J.J., Tsimring, L.S.: The Analysis of Observed Chaotic Data in Physical Systems. Rev. Mod. Phys. **65** (1993) 1331–1392